



Research Article

Implementation of New Stepped Square Pyramid Solar Still for Desalinating Seawater in The Climate of Upper Egypt

Ahmed H. Mohammed ^{a*}, Ahmed N. Shmroukh ^{a,b}, Nouby M. Ghazaly ^{a,c}, Abd Elnaby Kabeel ^{d,e,f}

^a Department of Mechanical Engineering, Faculty of Engineering, South Valley University, P. O. Box: 8352, Qena, Egypt.

^b Faculty of Industry and Energy-Technology, New Cairo Technological University, P. O. Box: 11835, Cairo, Egypt.

^c Technical College, Imam Ja'afar Al-Sadiq University, Baghdad, Iraq.

^d Department of Mechanical Power Engineering, Faculty of Engineering, Tanta University, P. O. Box: 31521, Tanta, Egypt.

^e Faculty of Engineering, Delta University for Science and Technology, Gamasa, Egypt.

^f Department of Mechanical Engineering, Islamic University of Madinah, P. O. Box: 42351, Medina, Saudi Arabia.

PAPER INFO

Paper history:

Received: 14 December 2023

Revised: 28 February 2024

Accepted: 06 April 2024

Keywords:

Pyramid Solar Still,

Stepped Basins,

Yield,

Efficiency,

Cost Analysis

ABSTRACT

In the present study, a modified pyramid-solar-still (MPSS) with new multiple stepped basin areas was investigated in the weather conditions of Qena, Egypt, at a location of (Latitude: 26.16°, Longitude: 32.71°). Boosting the output of the pyramid solar still is the primary focus of the proposed strategy. To achieve this, four basins were built and integrated into the pyramid solar still, with their size increasing in proportion to the surface area of the condensing glass. A 25% increase in basin area per square meter of solar still was achieved compared to conventional pyramid solar still (CPSS) with the same condensing cover area. The thermal performance and productivity of the suggested solar still were demonstrated by developing energy balance equations for temperature components and then analytically computing their solutions. The results showed compatibility between theoretical and experimental results. The highest yields for CPSS were 2524 mL/m², and for MPSS, they were 3415 mL/m². The stepped area enhanced the yield by 35.3% compared with CPSS. Moreover, the efficiency of CPSS and MPSS was recorded as 23.5% and 31.7%, respectively. Furthermore, the maximum yield of freshwater was obtained for the northern condensing cover, with the recorded value reaching 1174 mL/m². Distilled water under the proposed system would cost \$0.0179 per liter. Finally, the TDS and pH levels are in accordance with WHO recommendations for the quality of drinking water.

<https://doi.org/10.30501/jree.2024.424544.1729>

1. INTRODUCTION

The importance of using solar distillation techniques to provide clean water to the public cannot be overstated. Despite their convenience and low cost, these distillation techniques have a low yield. New designs, shapes, and materials are employed to boost the rate of evaporation within stills and, in turn, increase the amount of freshwater that can be produced (A. Abdullah, Essa, & Omara, 2021; AlQdah et al., 2022). The most basic technique of solar distillation is the solar still, which provides drinkable water for remote communities and individual residences in dry places (Ahmed H. Mohammed, Attalla, & Shmroukh, 2021). The low output of traditional stills has piqued the curiosity of researchers looking for ways to maximize distillate yield via novel arrangements. Successful modifications include many combinations of designs and shapes that were investigated experimentally and theoretically (Ahmed H. Mohammed, Shmroukh, Ghazaly, & Kabeel, 2023a). Several studies have compared various pyramid solar still designs to find those that provide the highest distillate output with the least amount of wasted energy. Pyramid solar

stills are a tried-and-true method of making salty water potable (Saravanavel, Vijayakumar, SathishKumar, Meignanamoorthy, & Ravichandran, 2020). Many researchers investigated the triangular and square shapes of pyramid solar still. Most research into improving the still's efficiency has focused on various types of fins, energy storage materials, heat pipes, and wick materials (Al-Madhhachi & Smaism, 2021; Fallahzadeh, Aref, Gholamirjenaki, Nonejad, & Saghi, 2020; Javad Raji Asadabadi & Sheikholeslami, 2022; Kumar et al., 2017; Ahmed H. Mohammed, Shmroukh, Ghazaly, & Kabeel, 2023b; Saravanan & Murugan, 2020; Sathyamurthy, Kennady, Nagarajan, & Ahsan, 2014; Taamneh & Taamneh, 2012). (Al-Madhhachi & Smaism, 2021) built and tested a square pyramid-solar still at Al Kufa, Iraq, throughout four seasons, with a maximum production of 2.2 L/m². Moreover, (Kabeel, El-Maghlany, Abdelgaied, & Abdel-Aziz, 2020) investigated how the effectiveness of an MPSS was assessed by placing a PCM tank underneath the absorber surface and installing a hollow fin array at the basin plate. This configuration resulted in the highest daily output of 8.1L/day. Furthermore, (Fallahzadeh et al., 2020) combined a pyramid-shaped solar-

*Corresponding Author's Email: A.H.Mohammed@eng.svu.edu.eg (A. H. Mohammed)

URL: https://www.jree.ir/article_193963.html



still with solar collector and got a yield of 6.97 L/m². (Kabeel, Abdelgaied, & Almulla, 2016) examined how a square pyramid solar still's performance varied depending on the angle of its glass cover in Tanta, Egypt. The results showed that the cumulative water production was almost 4.13 L/m² per day for a tilted glass covering of 30.47°, 3.5 L/m² per day for a tilted glass covering of 40°, and 2.93 L/m² per day for a tilted glass covering of 50°. (Kabeel, Teamah, Abdelgaied, & Abdel Aziz, 2017) compared the distillate production of a solar still equipped with PCM to that of a conventional still (3.5 L/m²), and found that the latter produced around 6.6 L/m². Moreover, (A. S. Abdullah et al., 2023) tested a cords pyramidal solar still with a variety of fabrics functioning as burlap wicks and found that it was able to produce 8 liters per square meter each day. (Abdelgaied, Abdulla, Abdelaziz, & Kabeel, 2022) studied a modified stepped single slope solar still and achieved a yield of 9.79 L/m². Moreover, (Sharshir et al., 2022) evaluated trapezoidal pyramid solar still with reflector, and their results showed that the productivity of modified pyramid solar still reached up to 127.27% over that of the traditional one. (Elgendi et al., 2022) designed a pyramid-solar-still with automatic feed water. Changing the form of the glass cover and the basin area, which are two examples of the numerous methods and studies that have been conducted to increase solar still production (Ensafisoroor, Khamooshi, Egelioglu, & Parham, 2016; Khalili, Taheri, & Nourali, 2023; Parsa et al., 2022), includes using sponge (Arjunan, Aybar, & Nedunchezian, 2011), employing a double basin (Ayoub, Al-Hindi, & Malaeb, 2015; Suneja & Tiwari, 1999), examining the effect of wind speed (A.

A. El-Sebail, 2000), utilizing an air blower (Joy, Antony, & Anderson, 2018), exploring glass cover angle and thickness (Khalifa, 2011), and investigating water depth and free surface area (Kalidasa Murugavel, Chockalingam, & Srithar, 2008; A. K. Tiwari & Tiwari, 2006). A quick survey of the relevant literature reveals that past research has focused on studying how to improve solar stills via different means. Due to favorable climatic circumstances in Qena, Egypt, the current research, experimental assessment, and mathematical model of an MPSS with new stepped basin areas are conducted there. The primary goal of the suggested technique is to enhance the pyramid solar still output. To accomplish this, four basins were built and integrated into the pyramid solar still, with the size of each basin progressively decreasing as it moved closer to the condensing cover top. The overall basin surface per square meter of MPSS is 25% more than it would be in a CPSS with the same condensing cover area.

2. Methodology

The pyramid solar still was made from galvanized steel that was 2 mm thick. The shape of the black basin is square. The top of the basin is made of a 4-mm-thick acrylic cut at a 26-degree angle. The main reason for the selection of this angle is that the productivity of solar stills will reach its maximum at a cover tilt angle that is close to the latitude angle of the site, and the latitude of the test site is 26.16° (Khalifa, 2011), (Kabeel et al., 2016).

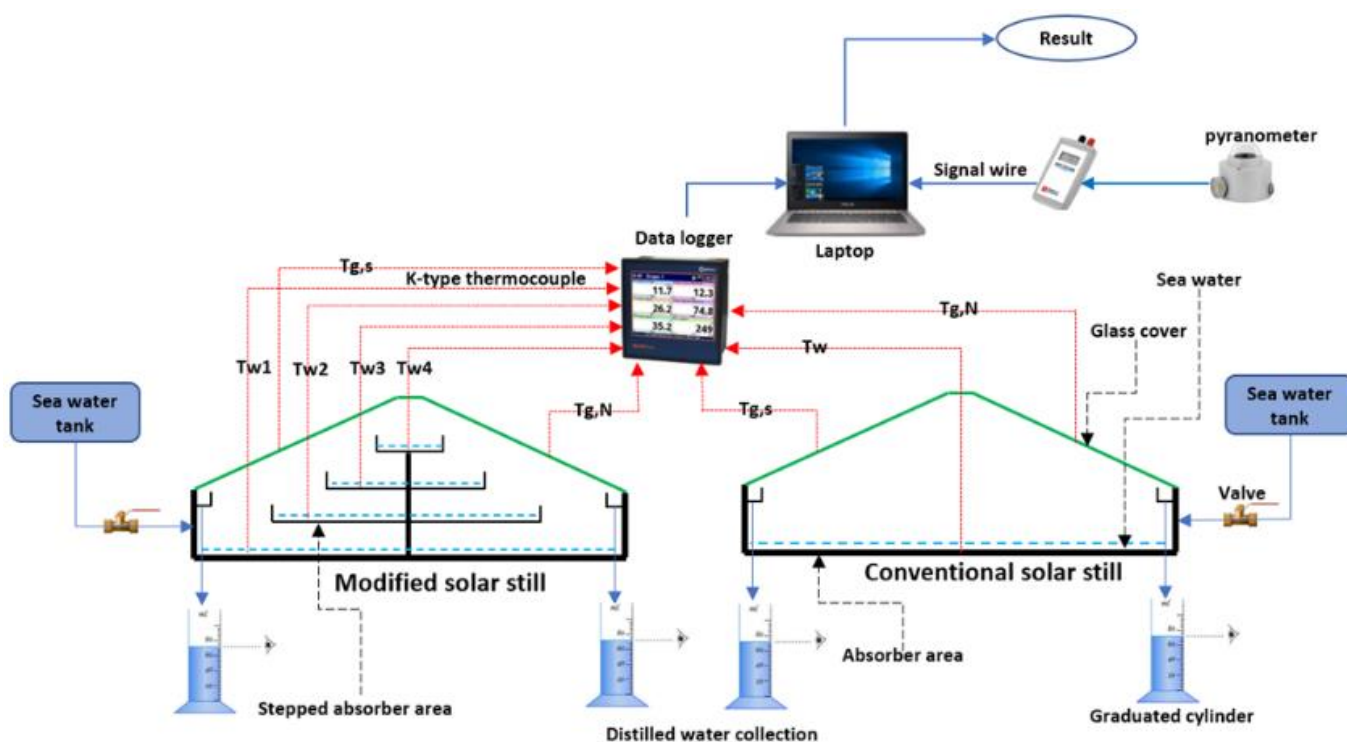


Figure 1. Schematic diagram of the proposed system.

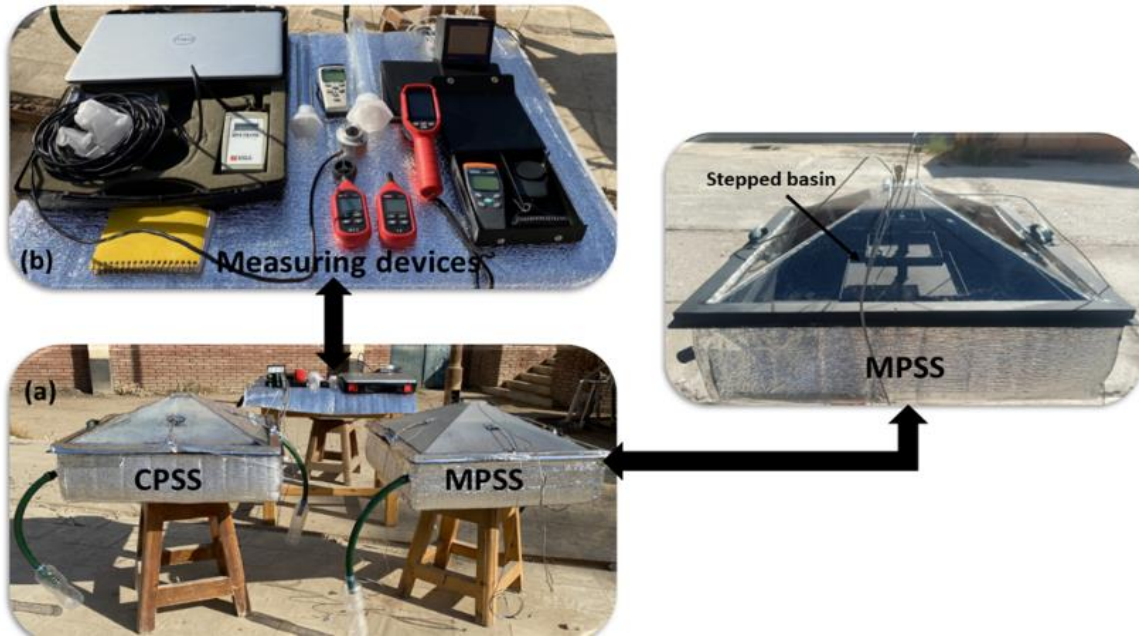


Figure 2. (a) Experimental test rig, (b) measuring devices.

The rough edges of the acrylic sheets were finished by welding four troughs onto each end. The distilled liquid was first collected in the troughs before being transferred to the proper storage vessels. Glass wool sheets were used to insulate the solar still and prevent heat loss via any of the connections on the sides or walls. A plastic pipe was used to transport the distillate from the two solar still collection sites to the waiting flasks. Two solar distillers, a saltwater storage tank, and other components are seen in Figure 1 and Figure 2. One solar distiller was the MPSS, while the other one served as a reference (CPSS). The MPSS consists of four stepped basins areas (surface 1; $0.6 \times 0.6 \text{ m}^2$, surface 2; $0.25 \times 0.25 \text{ m}^2$, surface 3; $0.15 \times 0.15 \text{ m}^2$, surface 4; $0.07 \times 0.07 \text{ m}^2$) with a total area of 0.4499 m^2 and four condensers, while the CPSS has a total area of 0.36 m^2 without any stepped area. The total seawater MPSS has been gradually divided among the four basins, and the amount of seawater inside each device was 10 L. The temperatures of the condensing cover, water, and ambient were measured by 14 K-type thermocouples. Additionally, the performance of the solar distillers was estimated using measurements of the solar irradiance, humidity, and distillate quantity, while each measurement was recorded hourly. Parameters, precision, and allowable margins of error for various pieces of measuring equipment used are detailed in Table 1. Finally, testing took place during the period from 9 a.m. to 6 p.m. The error analysis was employed using the following equation (Holman & Lloyd, 1955; A. H. Mohammed, Attalla, & Shmroukh, 2022).

$$\delta R = \sqrt{\left[\frac{\partial R}{\partial x_1} x_1\right]^2 + \left[\frac{\partial R}{\partial x_2} x_2\right]^2 + \dots + \left[\frac{\partial R}{\partial x_N} x_N\right]^2} \quad (1)$$

where x_1, x_2, \dots, x_N are the uncertainties of the independent parameters. Table 1 contains all computed tool errors.

Table 1. Measuring instruments specifications..

Instrument	Type	Dimension	units	Range and accuracy	Standard uncertainty
Thermocouple	K-type	Temperature	°C	-50 to 150, $\pm 0.5^\circ\text{C}$	$\pm 0.85^\circ\text{C}$
Digital pyranometer	CM4	Solar radiation	W/m^2	0 to 4000, $\pm 1 \text{ W/m}^2$	$\pm 0.54 \text{ W/m}^2$
Humidity meter	UT333	Humidity	%	0 to 100%, $\pm 5\% \text{ RH}$	$\pm 2.9\% \text{ RH}$
Graduated cylinder	Glass	Yield	L	0 to 3, $\pm 5 \text{ mL}$	$\pm 2.89 \text{ mL}$
Data logger	CMC-99	-----	-----	-----	-----

3. MATHEMATICAL MODEL OF THE SYSTEM

The MPSS heat flow is shown in Figure 3. This energy-balanced solution was calculated under the following conditions:

- a) There is currently no steam venting.
- b) Because of the sturdy framework, no warm air will escape.

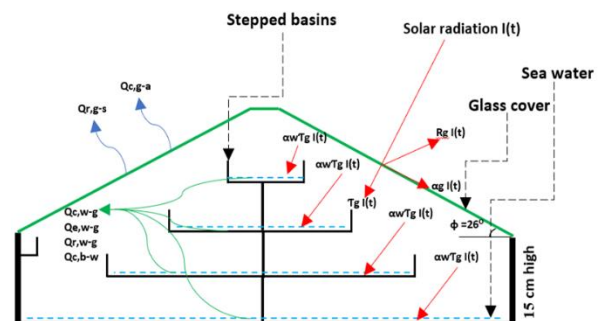


Figure 3. Schematic of the heat flow through the parts of MPSS.

The condensing coverings' energy-balance equation under steady-state conditions is expressed as (Alawee et al., 2021; A. El-Sebaei & Khallaf, 2020; Velmurugan et al., 2009):

$$I(t)A_g\alpha_g + Q_{c,w-g} + Q_{r,w-g} + Q_{e,w-g} = Q_{r,g-s} + Q_{c,g-s} \quad (2)$$

The water energy balance is (Alawee et al., 2021), (A. El-Sebaei & Khallaf, 2020):

$$I(t)A_w\alpha_w\tau_g + Q_{c,b-w} = m_w c p_w \frac{dT_w}{dt} + Q_{c,w-g} + Q_{r,w-g} + Q_{e,w-g} \quad (3)$$

The formula for the absorber's energy balance is (Alawee et al., 2021; A. El-Sebaei & Khallaf, 2020):

$$I(t)A_b\alpha_b\tau_g\tau_w = Q_{c,b-w} \quad (4)$$

where the water-basin-convective-heat-transfer is (Alawee et al., 2021; A. El-Sebaei & Khallaf, 2020):

$$Q_{c,b-w} = h_{c,b-w}A_b(T_b - T_w) \quad (5)$$

$h_{c,b-w}$ is determined by Ref. (Malaeb, Aboughali, & Ayoub, 2016)

$$h_{c,b-w} = 0.2 \left[\frac{k_w}{L} \right] Ra^{0.26} \quad (6)$$

(Ra) is the modified Rayleigh number.

$$Ra = \left[\frac{g \cdot \beta \cdot \rho_w \cdot L^3}{\mu_w \cdot D} \right] \cdot \Delta T' \quad (7)$$

β is the thermal expansion coefficient.

$$\beta = \frac{2}{T_b + T_w} \quad (8)$$

$$\text{And } \Delta T' = T_w - T_g + \frac{P_w - P_g}{268900 - P_w} \cdot T_w \quad (9)$$

Furthermore, the glass-water convective heat transfer is (Alawee et al., 2021; A. El-Sebaei & Khallaf, 2020):

$$Q_{c,w-g} = h_{c,w-g}A_w(T_w - T_g) \quad (10)$$

$h_{c,w-g}$ by (Kalidasa Murugavel, Sivakumar, Riaz Ahamed, Chockalingam, & Srithar, 2010).

$$h_{c,w-g} = 0.884 \left[T_w - T_g + \frac{P_w - P_g}{268900 - P_w} \cdot T_w \right]^{1/3} \quad (11)$$

where $P_{w,g}$ is partial pressure of water and glass is determined by Ref. (Malaeb et al., 2016).

$$P_{w,g} = \exp \left[25.317 - \frac{5144}{T_w \text{ or } g + 273} \right] \quad (12)$$

On the other hand, the water-glass radiative heat transfer.

$$Q_{r,w-g} = \sigma \varepsilon_g A_w \left[(T_w)^4 - (T_g)^4 \right] \quad (13)$$

$Q_{e,w-g}$ by (Omara, Eltawil, & ElNashar, 2013).

$$Q_{e,w-g} = h_{e,w-g}A_w(T_w - T_g) \quad (14)$$

where $h_{e,w-g}$ is

$$h_{e,w-g} = 0.016237 \cdot h_{c,w-g} \cdot \frac{P_w - P_g}{T_w - T_g} \quad (15)$$

Also, $Q_{r,g-s}$ by (Omara et al., 2013).

$$Q_{r,g-s} = h_{r,g-s}A_g(T_g - T_s) \quad (16)$$

where $h_{r,g-s}$ is

$$h_{r,g-s} = \varepsilon_g \sigma \frac{\left[(T_g)^4 - (T_s)^4 \right]}{(T_g - T_s)} \quad (17)$$

Finally, $Q_{c,g-s}$ by (Omara et al., 2013).

$$Q_{c,g-s} = h_{c,g-s}A_g(T_g - T_s) \quad (18)$$

where $h_{c,g-s}$ is (Sarhaddi, 2018).

$$h_{c,g-s} = 2.8 + 3V \text{ for } V \leq 5 \text{ m/s} \quad (19)$$

The hourly distillate is then determined by

$$\dot{m}_{ew} = \frac{h_{e,w-g}(T_w - T_g)}{h_{fg}} \quad (20)$$

The latent heat of vaporization defined by (Al-Kayiem, Mohamed, & Gilani, 2023; Essa, Alawee, Mohammed, Abdullah, & Omara, 2021; G. Tiwari & Sahota, 2017).

$$h_{fg} = 2.4935 \times 10^6 \left[1 - (9.4779 \times 10^{-4} \times T_w) + (1.3132 \times 10^{-7} \times T_w^2) - (4.7974 \times 10^{-9} \times T_w^3) \right] \quad (21)$$

Furthermore, the following relation was utilized to determine the thermal efficiency of the solar distiller (A. S. Abdullah et al., 2019).

$$\eta_d = \frac{\sum \dot{m}_{ew} \times h_{fg}}{\sum A \times I(t)} \quad (22)$$

Numerical simulations have been employed to hypothetically describe the square pyramid solar still with the following input parameters: The design parameters encompass the amount of leftover materials necessary to complete the pyramid, while climatic features comprise Qena's typical temperature and solar intensity in May 2023. Details regarding certain prerequisites for numerical calculations are outlined in Table 2.

Table 2. Numerical model's parameters (A. El-Sebaei & Khallaf, 2020).

Parameter	values	Parameter	values
k_{wa}	0.6405 (W/m.K)	τ_w	0.05
cp_{wa}	4190 (J/kg.K)	ε_g	0.88
α_g	0.05	α_b	0.95
α_w	0.95	σ	$5.6669 \times 10^{-8} \text{ w/m}^2 \cdot \text{k}^4$
τ_g	0.9	v	2 m/s for summer 3 m/s for winter

4. RESULTS AND DISCUSSION

4.1. Analysis of pyramid solar still

In Qena, Egypt, situated in the clear climate zone (Latitude: 26.16°, Longitude: 32.71°), experiments were conducted and studied for the suggested system from January to May of 2023. The fluctuations in solar radiation, outside temperature, and humidity over time are depicted in Figure 4. The figure illustrates that the intensity of solar output increases in the morning and peaks at 13:00, reaching 970.4 W/m². As the afternoon progresses, solar radiation gradually declines until it reaches its minimum value. The maximum ambient temperature and humidity recorded were 50.5°C and 25%, respectively. Figure 5 illustrates the variation between water and condensing cover temperatures in CPSS. The figure indicates that the maximum recorded basin water and condensing cover temperatures were 74°C and 66°C, respectively. Conversely, Figure 6 depicts the variation between water and condensing cover temperatures in MPSS. The maximum basin water and condensing cover temperatures

recorded were 79.5°C and 64°C, respectively. Furthermore, it is observed that the water-condensing cover temperature difference in MPSS was higher than in CPSS, leading to higher productivity in MPSS. All seawater in MPSS has been progressively distributed throughout its four basins. When the total quantity of saltwater is divided among the four basins, the total thermal capacity is divided accordingly, depending on the size of the evaporating water surface area in MPSS, which is larger than that of CPSS. The water in the four basins absorbs heat energy for evaporation significantly faster due to the division of thermal capacity. This results in increased productivity.

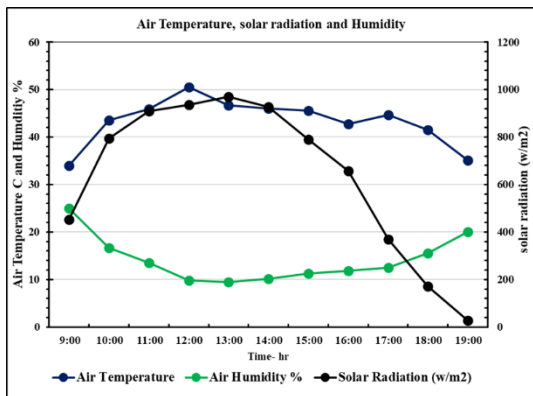


Figure 4. Variation between outside condition with time.

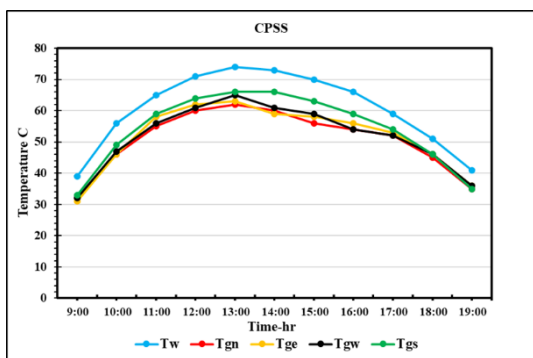


Figure 5. Variation between water and condensing cover temperatures in CPSS.

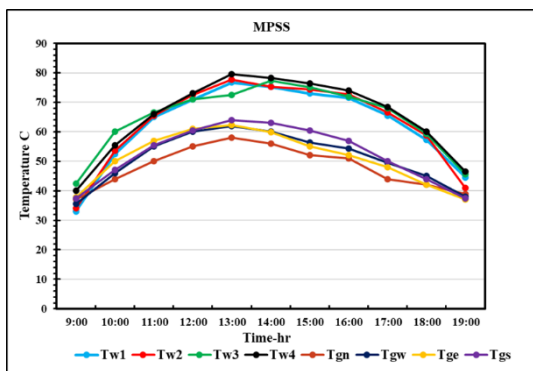


Figure 6. Variation between water and condensing cover temperatures in MPSS.

Figure 7 shows the variation in hourly yield between CPSS and MPSS over time. It is observed that the hourly yield of solar stills increases in the morning and reaches its maximum at 15:00 for both MPSS and CPSS, when it is 560 and 475 mL/m², respectively. As the afternoon progresses, the hourly yield progressively drops until it reaches its minimum value.

Moreover, Figure 8 illustrates the variation in accumulated yield between CPSS and MPSS over time. It is observed that the accumulated yield of MPSS is higher than that of CPSS, recording 3415 mL/m² and 2524 mL/m², respectively, representing an increase of 35.3% over CPSS. Furthermore, the enhancement in the daily yield of MPSS is reflected in the average daily efficiency of both solar stills, recorded at 23.5% and 31.7%, respectively. Due to the low thermal capacity of each basin, the distribution of water's thermal capacity throughout the four-stepped basins has increased the distillate yield and average daily efficiency.

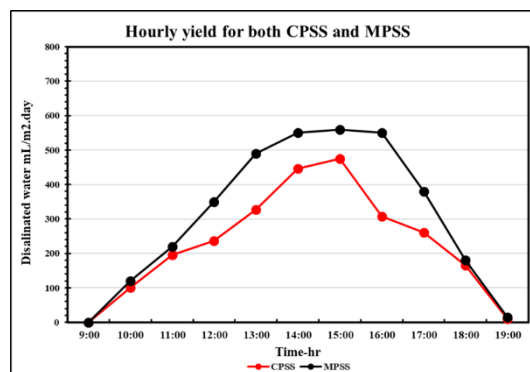


Figure 7. Variation between hourly yield in CPSS and MPSS with time.

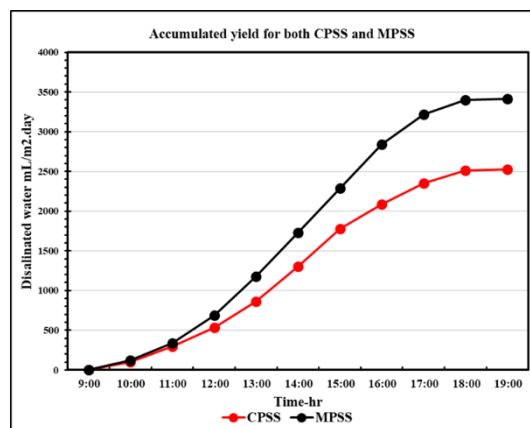


Figure 8. Variation between accumulated yield in CPSS and MPSS with time.

The hourly yield for MPSS and the analytical outcomes produced by the energy balance equation have been compared. Figure 9 illustrates the experimental/theoretical values of distillate output. The figure shows that there is compatibility between theoretical and experimental results. Analytical solutions for the hourly yield of freshwater are used to calculate the freshwater productivity for each condensing cover direction (East, West, South, and North). Figure 10 illustrates that the maximum yield of freshwater was gained for the northern condensing cover and recorded 1174 mL/m². This occurred because the condensing cover recorded the lowest temperature throughout the day as shown in Figure 6, which resulted in a higher temperature difference between the water and the condensing cover. It is important to increase and enhance the evaporation-and-condensation process inside the pyramid-solar-still. Finally, the TDS and pH levels for distilled water are in accordance with WHO recommendations for the quality of drinking water and were recorded at 122 ppm and 7.2, respectively.

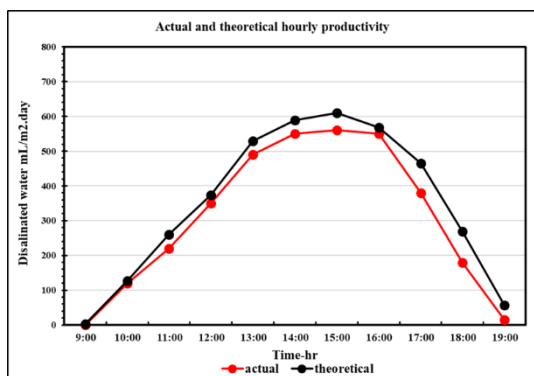


Figure 9. Theoretical/experimental results of distillate output.

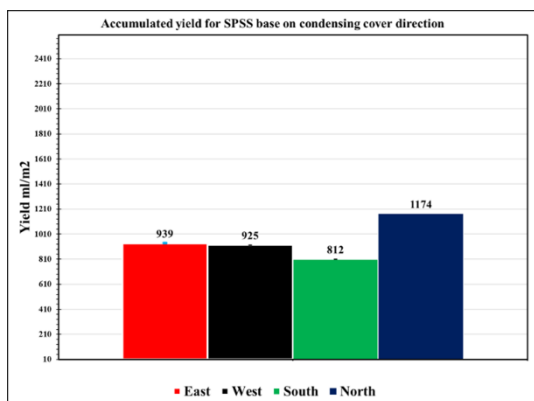


Figure 10. Maximum yield of freshwater based on condensing cover direction.

4.2. Economic analysis

A solar desalination unit's distillate production cost is influenced by several variables. The size of the unit, site location, feed-water characteristics, the quality of the product water required, and the availability of qualified employees are all factors that influence capital and operational costs, hence affecting the total cost (Abed & Hachim, 2021), (Fath, El-Samanoudy, Fahmy, & Hassabou, 2003; Singh & Sharma, 2022), (Ahanger Darabi et al., 2022).

$$CRF = \frac{i(1+i)^n}{(1+i)^n - 1} \quad (23)$$

Table 5. Comparison of the current study and previous literature.

Author	Method/ location	Yield/Increment %	Efficiency	CPL \$/L
(Saravanan & Murugan, 2020)	square pyramid-solar-still with various vertical wick materials.	33.1%	29.57%	N/A
(Kianifar, Zeinali Heris, & Mahian, 2012)	pyramid-solar-still with small fan	3.05	N/A	0.042
(Prakash & Jayaprakash, 2021)	pyramid solar still with stepped basins system.	3.25 L/day	50.85%	N/A
(Sathyamurthy, Nagarajan, Subramani, Vijayakumar, & Mohammed Ashraf Ali, 2014)	pyramid-solar-still with latent heat energy storage.	35%	N/A	N/A
(Kabeel et al., 2019)	pyramid-solar-still with the absorber plate coated with TiO ₂ nanoparticle mixed with black paint	6.25%	N/A	0.0107
Present study	Passive pyramid-solar-still with four stepped basins	35.3%	31.7%	0.0179

5. CONCLUSIONS

The experiments were carried out in Qena, Egypt. This paper includes a literature study, an experimental assessment, and a mathematical model of a modified pyramid-solar-still (MPSS) with a novel stepped basin area aimed at increasing

$$FAC = P \times CRF \quad (24)$$

$$SFF = \frac{i}{(1+i)^n - 1} \quad (25)$$

$$ASV = 0.2 \times P \times SFF \quad (26)$$

$$AMC = 0.15 \times FAC \quad (27)$$

$$AC = FAC + AMC - ASV \quad (28)$$

$$CPL = \frac{AC}{M} \quad (29)$$

where P is the upfront investment for the desalination system, *i* is the-interest rate each year (here, we'll estimate 12%), and n is the expected lifespan in years (10 for simplicity's sake). The breakdown of the system costs is given in Tables 3 and 4.

Table 3. Costs of the components of MPSS.

No	Components	Material	Cost (\$)
1	Transparent	Acrylic	65 \$
2	Absorber (basin)	galvanized iron	40 \$
3	Insulator	Glass wool	5 \$
4	Sealant	silicone rubber	3 \$
5	paint	Black paint	2 \$
6	Total cost (P)		115 \$

Table 4. Cost analysis result

1	CRF (Capital recovery factor)	0.177
2	FAC (Fixed annual cost)	20.355
3	SFF (Sinking fund factor)	0.057
4	P (Investment)	115
5	ASV (Annual salvage value)	1.311
6	AMC (Maintenance cost)	3.053
7	AC (Annual cost)	22.097
8	CPL (Cost of distilled water per liter)	0.0179

4.2. A comparison between the current study and previous literature

Table 5 displays the similarities and differences between the current experimental work and relevant works found in the public domain. The current findings are compared to those of five previous research studies in the table below.

freshwater production. The following are conclusions drawn from the research:

- This study demonstrated that evaporation might be increased by using a stepped basin solar still to decrease the still's internal heat capacity.

- There is compatibility between theoretical and experimental results. The maximum yield of freshwater was achieved with the northern condensing cover, recording 1174 mL/m².
- The maximum yield of CPSS and MPSS recorded 2524 and 3415 mL/m², respectively. The stepped area enhanced the yield by 35.3% over the CPSS.
- Average daily efficiency for the CPSS is 23.5%, whereas for the MPSS it is 31.7%.
- Distilled water under the proposed system would cost 0.0179 \$ per liter.
- Finally, the TDS and pH levels are in accordance with WHO recommendations for the quality of drinking water.

6. ACKNOWLEDGEMENT

The authors are very thankful to the Research Center, Imam Ja'afar Al-Sadiq University, Iraq, and South Valley University, Egypt, for providing a good research environment and services.

NOMENCLATURE

A	Area [m ²]
C _p	Specific-heat [J/kg.K]
g	Gravity [m/s ²]
h _{fg}	Latent-heat [J/kg.k]
I(t)	Average-solar-radiation [W/m ²]
m'	Yield [L/m ² .day]
m	Mass [kg]
L	Characteristic length [m]
N	Set of measured values [-]
P	Partial vapor pressure [N/m ²]
Q	Heat transfer rate [J]
Ra	Rayleigh number
Greek letters	
α	Absorptivity
β	Thermal expansion coefficient
ε	Emissivity [-]
∞	ambient condition
Subscripts	
a	Ambient
b	Basin
c	Convective
E	Eastern
e	Evaporative
g	Condensing cover
N	Northern
r	Radiative
S	Southern
s	Sky
w	Water
W	Western

REFERENCES

1. Abdelgaied, M., Abdulla, A. S., Abdelaziz, G. B., & Kabeel, A. E. (2022). Performance improvement of modified stepped solar distillers using three effective hybrid optimization modifications. *Sustainable Energy Technologies and Assessments*, 51, 101936. <https://doi.org/10.1016/j.seta.2021.101936>
2. Abdullah, A., Essa, F., & Omara, Z. (2021). Effect of different wick materials on solar still performance—a review. *International Journal of Ambient Energy*, 42(9), 1055-1082. <https://doi.org/10.1080/01430750.2018.1563808>
3. Abdullah, A. S., Alawee, W. H., Mohammed, S. A., Majdi, A., Omara, Z. M., & Essa, F. A. (2023). Increasing the productivity of modified cords pyramid solar still using electric heater and various wick materials. *Process Safety and Environmental Protection*, 169, 169-176. <https://doi.org/10.1016/j.psep.2022.11.016>
4. Abdullah, A. S., Essa, F. A., Omara, Z. M., Rashid, Y., Hadj-Taieb, L., Abdelaziz, G. B., & Kabeel, A. E. (2019). Rotating-drum solar still with enhanced evaporation and condensation techniques: Comprehensive study. *Energy Conversion and Management*, 199, 112024. <https://doi.org/10.1016/j.enconman.2019.112024>
5. Abed, Q. A., & Hachim, D. M. (2021). Enhancing the Productivity of Tubular Solar Still by Using the Phase Change Material. *Arabian Journal for Science and Engineering*, 46(12), 11645-11660. <https://doi.org/10.1007/s13369-021-05561-3>
6. Ahangar Darabi, M., Pasha, G., Ebrahimpour, B., Guodarzi, A. M., Morshedsolouk, F., Habibnejad Roshan, H., & Shafaghat, R. (2022). Experimental investigation of a novel single-slope tilted wick solar still with an affordable channelled absorber sheet, an external condenser, and a reflector. *Solar Energy*, 241, 650-659. <https://doi.org/10.1016/j.solener.2022.06.020>
7. Al-Kayiem, H. H., Mohamed, M. M., & Gilani, S. I. U. (2023). State of the Art of Hybrid Solar Stills for Desalination. *Arabian Journal for Science and Engineering*, 48(5), 5709-5755. <https://doi.org/10.1007/s13369-022-07516-8>
8. Al-Madhachi, H., & Smaism, G. F. (2021). Experimental and numerical investigations with environmental impacts of affordable square pyramid solar still. *Solar Energy*, 216, 303-314. <https://doi.org/10.1016/j.solener.2020.12.051>
9. Alawee, W. H., Essa, F., Mohammed, S. A., Dhahad, H. A., Abdullah, A., Omara, Z., & Gamiel, Y. (2021). Improving the performance of pyramid solar distiller using dangled cords of various wick materials: novel working mechanism of wick. *Case Studies in Thermal Engineering*, 28, 101550. <https://doi.org/10.1016/j.csite.2021.101550>
10. AlQdah, K. S., Alharbi, K. A., Alharbi, S. A., Almutairi, M. A., Alsuheimi, O. M., & Aljuhani, M. S. (2022). Design, Fabrication and Performance Evaluation of a Semi-Cylindrical Solar Still Working in Medina Region. *Arabian Journal for Science and Engineering*, 47(7), 8567-8575. <https://doi.org/10.1007/s13369-021-06351-7>
11. Arjunan, T. V., Aybar, H. Ş., & Nedunchezian, N. (2011). Effect of sponge liner on the internal heat transfer coefficients in a simple solar still. *Desalination and Water Treatment*, 29(1-3), 271-284. <https://doi.org/10.5004/dwt.2011.1638>
12. Ayoub, G. M., Al-Hindi, M., & Malaeb, L. (2015). A solar still desalination system with enhanced productivity. *Desalination and Water Treatment*, 53(12), 3179-3186. <https://doi.org/10.1080/19443994.2014.933040>
13. El-Sebaai, A., & Khallaf, A. E. (2020). Mathematical modeling and experimental validation for square pyramid solar still. *Environ Sci Pollut Res Int*, 27(26), 32283-32295. <https://doi.org/10.1007/s11356-019-07587-5>
14. El-Sebaai, A. A. (2000). Effect of wind speed on some designs of solar stills. *Energy Conversion and Management*, 41(6), 523-538. [https://doi.org/10.1016/S0196-8904\(99\)00119-3](https://doi.org/10.1016/S0196-8904(99)00119-3)
15. Elgendi, M., Selim, M. Y. E., Aldhaheri, A., Alshehhi, W., Almarshoodi, H., & Alhefeiti, A. (2022). Design procedures for a passive pyramid solar still with an automatic feed water system. *Alexandria Engineering Journal*, 61(8), 6419-6431. <https://doi.org/10.1016/j.aej.2021.12.002>
16. Ensafisoroor, H., Khamooshi, M., Egelioglu, F., & Parham, K. (2016). An experimental comparative study on different configurations of basin solar still. *Desalination and Water Treatment*, 57(5), 1901-1916. <https://doi.org/10.1080/19443994.2014.979238>
17. Essa, F. A., Alawee, W. H., Mohammed, S. A., Abdullah, A. S., & Omara, Z. M. (2021). Enhancement of pyramid solar distiller performance using reflectors, cooling cycle, and dangled cords of wicks. *Desalination*, 506, 115019. <https://doi.org/10.1016/j.desal.2021.115019>
18. Fallahzadeh, R., Aref, L., Gholamirjenaki, N., Nonejad, Z., & Saghi, M. (2020). Experimental investigation of the effect of using water and ethanol as working fluid on the performance of pyramid-shaped solar still integrated with heat pipe solar collector. *Solar Energy*, 207, 10-21. <https://doi.org/10.1016/j.solener.2020.06.032>
19. Fath, H. E. S., El-Samanoudy, M., Fahmy, K., & Hassabou, A. (2003). Thermal-economic analysis and comparison between pyramid-shaped and single-slope solar still configurations. *Desalination*, 159(1), 69-79. [https://doi.org/10.1016/S0011-9164\(03\)90046-4](https://doi.org/10.1016/S0011-9164(03)90046-4)
20. Holman, J. P., & Lloyd, J. R. (1955). *McGraw-Hill series in mechanical engineering*: MacGraw-Hill.
21. Javad Raji Asadabadi, M., & Sheikholeslami, M. (2022). Impact of utilizing hollow copper circular fins and glass wool insulation on the performance enhancement of pyramid solar still unit: An experimental

- approach. *Solar Energy*, 241, 564-575. <https://doi.org/10.1016/j.solener.2022.06.029>
22. Joy, N., Antony, A., & Anderson, A. (2018). Experimental study on improving the performance of solar still using air blower. *International Journal of Ambient Energy*, 39(6), 613-616. <https://doi.org/10.1080/01430750.2017.1324817>
 23. Kabeel, A. E., Abdelgaied, M., & Almulla, N. (2016, 22-24 March 2016). *Performances of pyramid-shaped solar still with different glass cover angles: Experimental study*. Paper presented at the 2016 7th International Renewable Energy Congress (IREC). <https://doi.org/10.1109/IREC.2016.7478869>
 24. Kabeel, A. E., El-Maghlany, W. M., Abdelgaied, M., & Abdel-Aziz, M. M. (2020). Performance enhancement of pyramid-shaped solar stills using hollow circular fins and phase change materials. *Journal of Energy Storage*, 31, 101610. <https://doi.org/10.1016/j.est.2020.101610>
 25. Kabeel, A. E., Sathyamurthy, R., Sharshir, S. W., Muthumanokar, A., Panchal, H., Prakash, N., El Kady, M. S. (2019). Effect of water depth on a novel absorber plate of pyramid solar still coated with TiO₂ nano black paint. *Journal of Cleaner Production*, 213, 185-191. <https://doi.org/10.1016/j.jclepro.2018.12.185>
 26. Kabeel, A. E., Teamah, M. A., Abdelgaied, M., & Abdel Aziz, G. B. (2017). Modified pyramid solar still with v-corrugated absorber plate and PCM as a thermal storage medium. *Journal of Cleaner Production*, 161, 881-887. <https://doi.org/10.1016/j.jclepro.2017.05.195>
 27. Kalidasa Murugavel, K., Chockalingam, K. K. S. K., & Srithar, K. (2008). An experimental study on single basin double slope simulation solar still with thin layer of water in the basin. *Desalination*, 220(1), 687-693. <https://doi.org/10.1016/j.desal.2007.01.063>
 28. Kalidasa Murugavel, K., Sivakumar, S., Riaz Ahamed, J., Chockalingam, K. K. S. K., & Srithar, K. (2010). Single basin double slope solar still with minimum basin depth and energy storing materials. *Applied Energy*, 87(2), 514-523. <https://doi.org/10.1016/j.apenergy.2009.07.023>
 29. Khalifa, A. J. N. (2011). On the effect of cover tilt angle of the simple solar still on its productivity in different seasons and latitudes. *Energy Conversion and Management*, 52(1), 431-436. <https://doi.org/10.1016/j.enconman.2010.07.018>
 30. Khalili, M., Taheri, M., & Nourali, A. (2023). Metal fins efficacy on stepped solar still performance: An experimental study. *Desalination*, 563, 116706. <https://doi.org/10.1016/j.desal.2023.116706>
 31. Kianifar, A., Zeinali Heris, S., & Mahian, O. (2012). Exergy and economic analysis of a pyramid-shaped solar water purification system: Active and passive cases. *Energy*, 38(1), 31-36. <https://doi.org/10.1016/j.energy.2011.12.046>
 32. Kumar, P. N., Manokar, A. M., Madhu, B., Kabeel, A. E., Arunkumar, T., Panchal, H., & Sathyamurthy, R. (2017). Experimental investigation on the effect of water mass in triangular pyramid solar still integrated to inclined solar still. *Groundwater for Sustainable Development*, 5, 229-234. <https://doi.org/10.1016/j.gsd.2017.08.003>
 33. Malaeb, L., Aboughali, K., & Ayoub, G. M. (2016). Modeling of a modified solar still system with enhanced productivity. *Solar Energy*, 125, 360-372. <https://doi.org/10.1016/j.solener.2015.12.025>
 34. Mohammed, A. H., Attalla, M., & Shmroukh, A. N. (2021). Performance enhancement of single-slope solar still using phase change materials. *Environmental Science and Pollution Research*, 28(14), 17098-17108. <https://doi.org/10.1007/s11356-020-12096-x>
 35. Mohammed, A. H., Attalla, M., & Shmroukh, A. N. (2022). Comparative study on the performance of solar still equipped with local clay as an energy storage material. *Environ Sci Pollut Res Int*, 29(49), 74998-75012. <https://doi.org/10.1007/s11356-022-21095-z>
 36. Mohammed, A. H., Shmroukh, A. N., Ghazaly, N. M., & Kabeel, A. E. (2023a). Active solar still with solar concentrating systems, Review. *Journal of Thermal Analysis and Calorimetry*, 148(17), 8777-8792. <https://doi.org/10.1007/s10973-023-12285-z>
 37. Mohammed, A. H., Shmroukh, A. N., Ghazaly, N. M., & Kabeel, A. E. (2023b). Performance evaluation and optimization of solar dish concentrator in the upper Egypt region. *Environmental Progress & Sustainable Energy*, n/a(n/a), e14325. <https://doi.org/10.1002/ep.14325>
 38. Omara, Z. M., Eltawil, M. A., & ElNashar, E. A. (2013). A new hybrid desalination system using wicks/solar still and evacuated solar water heater. *Desalination*, 325, 56-64. <https://doi.org/10.1016/j.desal.2013.06.024>
 39. Parsa, S. M., Yazdani, A., Javadi, D., Afrand, M., Karimi, N., & Ali, H. M. (2022). Selecting efficient side of thermoelectric in pyramid-shape solar desalination units incorporated phase change material (PCM), nanoparticle, turbulator with battery storage powered by photovoltaic. *Journal of Energy Storage*, 51, 104448. <https://doi.org/10.1016/j.est.2022.104448>
 40. Prakash, A., & Jayaprakash, R. (2021). Performance evaluation of stepped multiple basin pyramid solar still. *Materials Today: Proceedings*, 45, 1950-1956. <https://doi.org/10.1016/j.matpr.2020.09.227>
 41. Saravanan, A., & Murugan, M. (2020). Performance evaluation of square pyramid solar still with various vertical wick materials – An experimental approach. *Thermal Science and Engineering Progress*, 19, 100581. <https://doi.org/10.1016/j.tsep.2020.100581>
 42. Saravanel, S., Vijayakumar, K., SathishKumar, G. B., Meignanamoorthy, M., & Ravichandran, M. (2020). WITHDRAWN: Performance on single basin square pyramid solar still. *Materials Today: Proceedings*. <https://doi.org/10.1016/j.matpr.2020.10.943>
 43. Sarhaddi, F. (2018). Exergy analysis of a weir-type cascade solar still connected to PV/T collectors. *12(12)*, 1336-1344. <https://doi.org/10.1049/iet-rpg.2018.5162>
 44. Sathyamurthy, R., Kennady, H. J., Nagarajan, P. K., & Ahsan, A. (2014). Factors affecting the performance of triangular pyramid solar still. *Desalination*, 344, 383-390. <https://doi.org/10.1016/j.desal.2014.04.005>
 45. Sathyamurthy, R., Nagarajan, P. K., Subramani, J., Vijayakumar, D., & Mohammed Ashraf Ali, K. (2014). Effect of Water Mass on Triangular Pyramid Solar Still Using Phase Change Material as Storage Medium. *Energy Procedia*, 61, 2224-2228. <https://doi.org/10.1016/j.egypro.2014.12.114>
 46. Sharshir, S. W., Rozza, M. A., Elsharkawy, M., Youns, M. M., Abou-Taleb, F., & Kabeel, A. E. (2022). Performance evaluation of a modified pyramid solar still employing wick, reflectors, glass cooling and TiO₂ nanomaterial. *Desalination*, 539, 115939. <https://doi.org/10.1016/j.desal.2022.115939>
 47. Singh, D., & Sharma, A. K. (2022). Experimental Performance of Modified Multi-Wick Basin-Type Inverted Absorber Solar Still. *Arabian Journal for Science and Engineering*, 47(7), 8551-8565. <https://doi.org/10.1007/s13369-021-06320-0>
 48. Suneja, S., & Tiwari, G. N. (1999). Effect of water depth on the performance of an inverted absorber double basin solar still. *Energy Conversion and Management*, 40(17), 1885-1897. [https://doi.org/10.1016/S0196-8904\(99\)00047-3](https://doi.org/10.1016/S0196-8904(99)00047-3)
 49. Taamneh, Y., & Taamneh, M. M. (2012). Performance of pyramid-shaped solar still: Experimental study. *Desalination*, 291, 65-68. <https://doi.org/10.1016/j.desal.2012.01.026>
 50. Tiwari, A. K., & Tiwari, G. N. (2006). Effect of water depths on heat and mass transfer in a passive solar still: in summer climatic condition. *Desalination*, 195(1), 78-94. <https://doi.org/10.1016/j.desal.2005.11.014>
 51. Tiwari, G., & Sahota, L. (2017). *Advanced solar-distillation systems: basic principles, thermal modeling, and its application*: Springer. <http://dx.doi.org/10.1007/978-981-10-4672-8>
 52. Velmurugan, V., Pandiarajan, S., Guruparan, P., Subramanian, L. H., Prabakaran, C. D., & Srithar, K. (2009). Integrated performance of stepped and single basin solar stills with mini solar pond. *Desalination*, 249(3), 902-909. <https://doi.org/10.1016/j.desal.2009.06.070>